

Article

Optimal Hybridization with Minimum Fuel Consumption of the Hybrid Fuel Cell Train

Mario Mišić ^{1,*} , Marinko Stojkov ¹, Rudolf Tomić ² and Mario Lovrić ¹¹ Mechanical Engineering Faculty, University of Slavonski Brod, 35000 Slavonski Brod, Croatia² Faculty of Mechanical Engineering and Naval Architecture, University of Zagreb, 10000 Zagreb, Croatia

* Correspondence: mario.misic@yahoo.com

Abstract: This paper describes a numerical study of the optimal distribution of energy between fuel cells and auxiliary energy storages in the hybrid train. Internal combustion engines (ICEs) are currently under pressure from environmental agencies due to their harmful gas emissions, and pure battery vehicles have a short range; a hybrid train powered by fuel cells, batteries, and supercapacitors can provide a viable propulsion solution. In this study, special energy management on the mountain railway with optimal power distribution and minimum hydrogen consumption is proposed. Considering the characteristics of the mountain railway, the vehicle uses recuperation of regenerative braking energy and thus charges additional power devices, and hybridization optimization gives favorable power to each power source device with a minimum consumption of hydrogen in the fuel cell. In this study, a simulation model was created in a Matlab/Simulink environment for the optimization of hybridized power systems on trains, and it can be easily modified for the hybridization of any type of train. Optimization was performed by using Sequential quadratic programming (SQP). The results show that this hybrid train topology has the ability to recover battery and supercapacitor state of charge (SOC) while meeting vehicle speed and propulsion power requirements. The effect of battery and supercapacitor parameters on power distribution and fuel consumption was also simulated.

Keywords: optimization; hybridization; train; fuel cells; power management; SQP



Citation: Mišić, M.; Stojkov, M.; Tomić, R.; Lovrić, M. Optimal Hybridization with Minimum Fuel Consumption of the Hybrid Fuel Cell Train. *Designs* **2023**, *7*, 45. <https://doi.org/10.3390/designs7020045>

Academic Editors: Wenbin Yu and Guang Zeng

Received: 3 February 2023

Revised: 10 March 2023

Accepted: 13 March 2023

Published: 16 March 2023



Copyright: © 2023 by the authors. Licensee MDPI, Basel, Switzerland. This article is an open access article distributed under the terms and conditions of the Creative Commons Attribution (CC BY) license (<https://creativecommons.org/licenses/by/4.0/>).

1. Introduction

Since greenhouse gases have a great impact on the environment, various measures are being taken to reduce or perhaps even eliminate harmful emissions of exhaust gases. Trains are not big polluters in themselves [1], but limits for harmful gas emissions are still prescribed for diesel trains by Leaflet UIC624 (Table 1).

In order to decrease or completely eliminate the harmful emission of exhaust gases, hybrid vehicles powered by a fuel cell can be introduced [2,3]. Such vehicles do not pollute the environment, unlike diesel vehicles, and compared to pure battery vehicles, they have a much longer range.

The advantages of introducing hybrid fuel cell trains are:

- Zero harmful emissions of exhaust gases;
- Energy savings by recuperation of regenerative braking;
- Reduced mass of all power sources;
- Optimal power distribution on each auxiliary power source.

Hybrid vehicles can have numerous advantages over each individual component. A supercapacitor could enable instantaneous cold-start operation of auxiliary devices while the fuel cell warms up. If the temperature is not too low, the battery could run the train from the depot to the departure station during a cold start. A hybrid system can allow all drive components to be smaller in size and operate with greater efficiency since none would have to provide full load and capacity.

Table 1. UIC624 ICE Emission Standards [4].

Stage	Date	Power, <i>P</i> [kW]	Engine Speed, <i>r</i> [min ⁻¹]	CO	HC	NOx	PM	Smoke
				g/kWh				
UIC I	up to 31 December 2002			3	0.8	12	-	1.6–2.5 ^a
UIC II	1 January 2003	<i>P</i> ≤ 560		2.5	0.6	6.0	0.25	
		<i>P</i> > 560	<i>r</i> > 1000	3	0.8	9.5	0.25 ^b	
			<i>r</i> ≤ 1000	3	0.8	9.9	0.25 ^b	

^a—Bosch smoke number (BSN) = 1.6 for engines with an air throughput of above 1 kg/s; BSN = 2.5 for engines below 0.2 kg/s; linear BSN interpolation applies between these 2 values. ^b—For engines above 2200 kW, a PM emission of 0.5 g/kWh is accepted on an exceptional basis until 31 December 2004.

Fuel cells could have zero harmful emissions of exhaust gases only if the fuel is hydrogen. In general, fuel cells can also work with methanol, natural gas, and gasoline. Since such fuels, in addition to hydrogen, contain carbon, it is impossible to avoid the exhaust gas carbon dioxide. Since the aim of this paper is to achieve zero harmful emissions of exhaust gases, only hydrogen is considered as a fuel. When using hydrogen as fuel, a chemical process produces water and energy.

Software and algorithms for simulations and optimization can contribute significantly to research. Matlab software has already been used to develop train motion simulations with Object Oriented Programming (OOP). Research in [5] shows the movement of a train with optimal driving times, which was compared with the actual railway. It showed that the simulation is very effective and applicable for the research and application of train operations.

Likewise, ADVISOR software is also a good modeling and cost-effectiveness analysis tool that was used to introduce a fuel cell hybrid locomotive. According to the traction characteristics of the Indian WDM-7 locomotive and the fuel cell as the main power source, in a certain driving cycle, the dynamic performance of the hybrid system was verified using an advanced vehicle simulator [6].

Fuel cells, batteries, and supercapacitors are very expensive devices, and it is necessary to efficiently determine their hybridization ratios. The aim is to reduce the power of the fuel cell to the lowest value and to design the battery and supercapacitor with the lowest losses [7]. In ref. [8], the numerically verified methods of hybridization are presented, and thus the optimal values of the power source are selected.

The possibility of installing fuel cells in trains has already been researched [9]. In the mentioned paper, the operation of the shunting locomotive according to the actual working cycle is presented. Energy management and power distribution between power sources were developed but without optimization. Since the shunting locomotive has demanding work, it still works on a straight railway in shorter time intervals. This is a good template for simulating a train on a mountain railway and can still show better system performance.

Matlab-Simulink™ (M/S™) can also be used to develop tools such as TrEnO, which provides tools for optimizing total energy consumption [10]. The tool is also able to estimate the efficiency, power dissipation, and thermal behavior of the traction system components. It is used during the conceptual faze of train prototypes to optimize the overall traction and braking of trains on a given railway.

The SQP optimization tool is incorporated into the M/S™ environment [11]. One of the first steps is to model the train speed trajectory. The minimum energy consumption can be set as an optimization goal, and a trade-off between energy consumption and accuracy can be made using the train trajectory model [12].

In this study, the SQP algorithm is used to optimize the hybridization of power sources of the train [13]. The model uses SQP to find the optimal hybridization ratio between the fuel cell, the battery, and the supercapacitor according to the trajectory of the train movement on the mountain railway between Knin and Perković in Croatia. The simulation itself calculates the power of the fuel cell, battery, and supercapacitor according to the given load currents of each power source [14]. The aim is the lowest consumption of hydrogen in fuel cells [15].

The energy management developed in this paper is based on SOC control. It is designed to maintain the charge of the battery and supercapacitor with optimal values, and the design was developed based on the prototype of a passenger train and a mountain railway.

2. Materials and Methods

2.1. Model and Topology of the Train

The train model in this work is based on the HŽ7022 prototype train of Croatian Railways. The train’s propulsion system is modeled as a hybrid of a fuel cell (FC), battery, and supercapacitor.

A passenger train has a uniform demand for maximum power during acceleration and cruising for reduced power that must overcome the force of movement resistance. In order to analyze the electricity demand of the train, a typical timetable with a railway profile was set according to the real railway in Croatia between Knin and Perković [16].

The simulation model in M/STM calculates the traction power at the wheels according to the railway trajectory and calculates the distribution of total train power between the power sources. The traction system topology used in trains can be connected in series or in parallel. The traction hybrid system for this train is connected in series [17] (Figure 1). Induction motors are connected to an IGBT (insulated gate bipolar transistor) converter that is connected to DC/DC converters that are directly connected to power sources [18]. The battery and supercapacitor are connected to bidirectional DC/DC converters for charging/discharging, while FC is connected to a chopper, a converter in one direction [19].

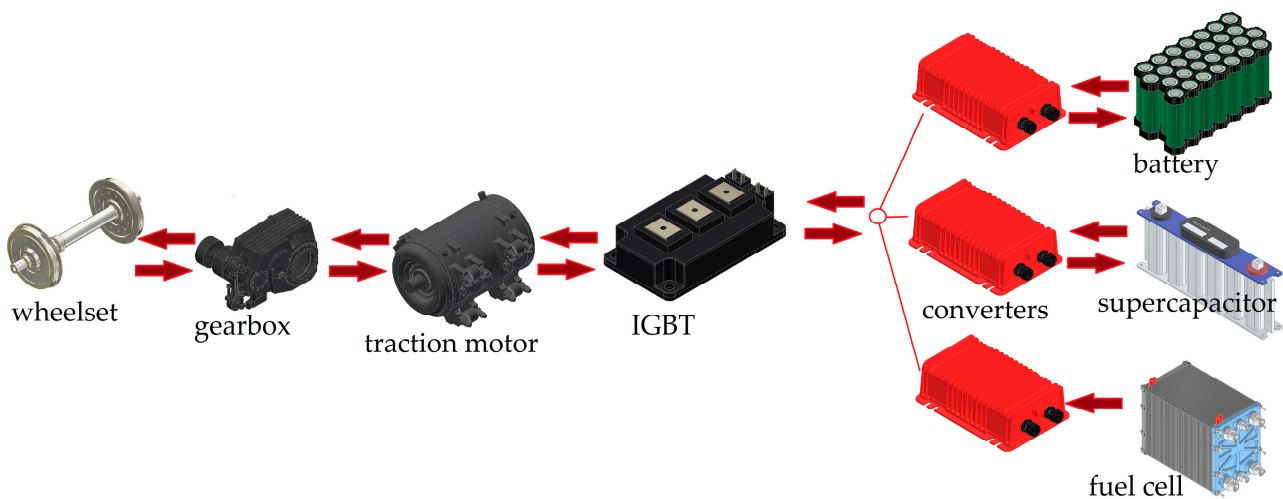


Figure 1. Power flow according to traction system topology.

According to the existing DMU (diesel multiple unit) train that will be converted into a hybrid fuel cell train, the maximum traction power is 1255 kW, and the maximum traction force is 125 kN. In a hybrid fuel cell train, the total power will be obtained from the fuel cell and auxiliary energy storage devices and taken over by the IGBT. The voltage on the IGBT is 2.4 kV, which is provided by the converters of power devices that receive a voltage of 0.8 kV. Such a high voltage generally corresponds well to the requirements of the drive system and enables lower losses in the power system.

The advantage of such a parallel system is the different voltages of the power sources. Each power source can work at its nominal voltage because the converter will raise the voltage to 2.4 kV, which is necessary for IGBT. However, it is desirable that the voltages of all power sources are approximately the same and as high as possible because the losses will be the lowest.

2.2. Energy Management System

The power flow passes with losses, and the energy management coordinates the operation of power devices and distributes the power to devices according to the hybridization ratio (Figure 2). When accelerating, energy management uses a fuel cell, battery, and supercapacitor for traction. For cruising, the supercapacitor performs traction until a state of charge $SOC_{sc} = 0.01$, and then the battery is used. If, during acceleration and cruising, the climb is greater than 15%, all devices are switched on. If $SOC_b = 0.2$, traction is performed by supercapacitor, and fuel cell will charge the battery. The battery drives the traction only after the supercapacitor is discharged ($SOC_{sc} = 0.01$). Regenerative braking will first charge the supercapacitor to $SOC_{sc} = 1$, and the battery only will be charged after supercapacitor is fully charged. Energy management does not allow $SOC_b = 0.2$ and $SOC_{sc} = 0.01$ at the same time.

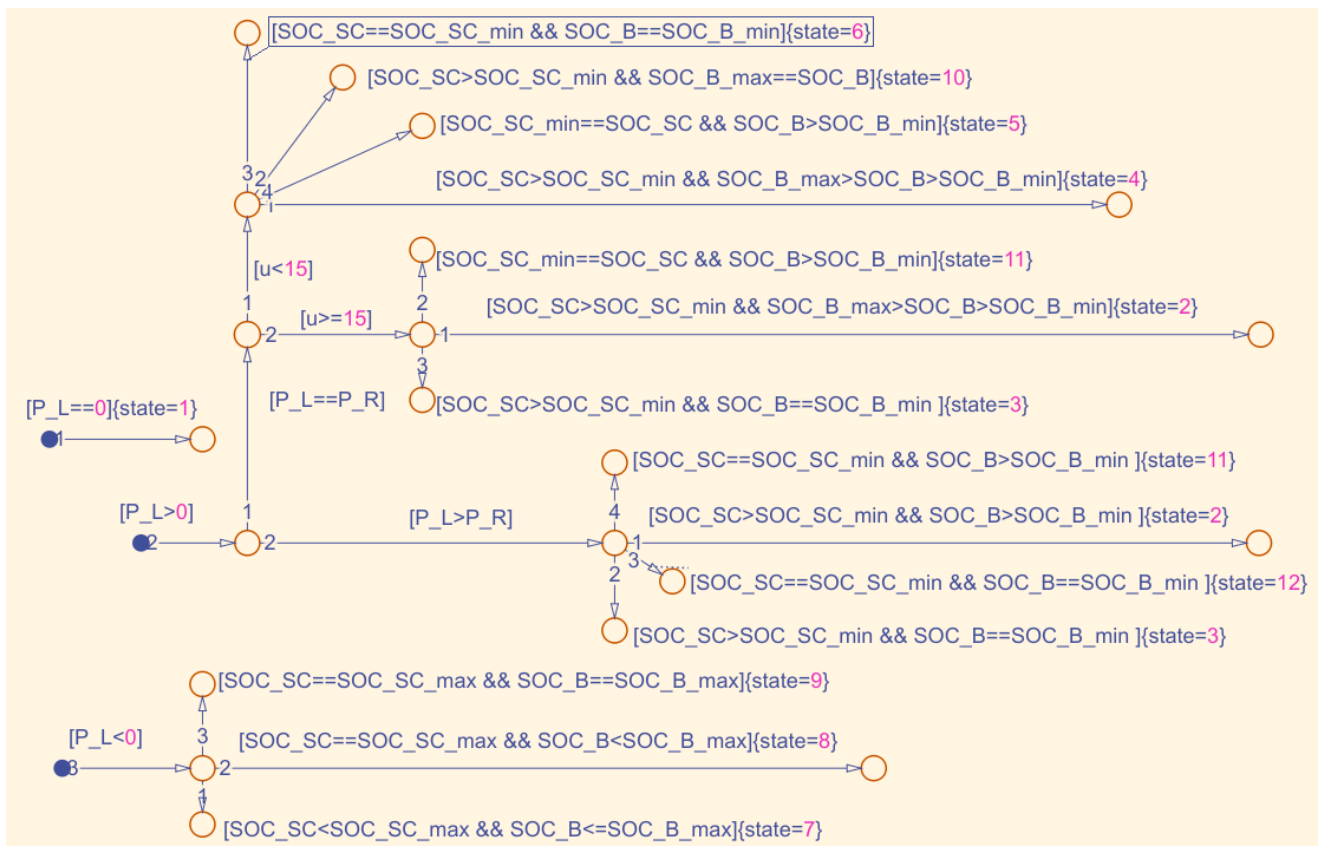


Figure 2. Energy management.

The hybridization ratio is affected by the total power, the properties of the railway, and the strength of the discharge currents of the fuel cell, battery, and supercapacitor.

2.3. Traction Force

Total power of the train is calculated as

$$P_{tot} = F_{tot} \cdot v_{tr} = (P_{fc} \cdot \eta_{fc} \cdot \eta_{dc} + P_b \cdot \eta_{dc} + P_{sc} \cdot \eta_{dc}) \cdot \eta_{ti} \cdot \eta_{tm} \cdot \eta_{gb}, \quad (1)$$

where F_{tot} is the total force for movement in N, v_{tr} is the train speed in m/s, P_{fc} is the fuel cell power in W, η_{fc} is the fuel cell efficiency, η_{dc} is the DC/DC converter efficiency, P_b is the battery power in W, P_{sc} is the supercapacitor power in W, η_{ti} is the traction inverter efficiency, η_{tm} is the traction motor efficiency, and η_{gi} is the gear box efficiency. For regenerative braking, each efficiency is calculated reciprocally ($1/\eta$), except for the fuel cell.

The total power (the total force) must be sufficient to overcome all resistances of the train:

$$F_{tot} \cdot a = F_{tr,max} - F_{dr} - F_{gr} - F_{cu} \tag{2}$$

$$a = \pm \frac{1}{m_{tot}} (F_{tr,max} - (r_{rr} + r_{pm} \cdot v_{tr} + r_{ar} \cdot v_{tr}^2)) - g \cdot (g_{rt} + \frac{0.5g}{R - 30}), \tag{3}$$

$$v_{tr} = \int a dt, \tag{4}$$

where F_{tr} is the traction force on wheels in N (positive for traction, negative for braking); m_{tot} is the total mass of the train in kg, increased by 6% due to the inertia of the rotating masses [20]; r_{rr} is the rolling resistance force in N; r_{pm} is the resistance coefficient of parasitic movements in N/kmh^{-1} ; r_{ar} is the air resistance coefficient in $N/(kmh^{-1})^2$; v_{tr} is the train speed in km/h; g is the gravitational acceleration; g_{rt} is the gradient of the railway in ‰; and R is the radius of curvature of the railway in m.

The traction force of the train is achieved up to the critical speed through torque, and after that, through the power of the traction motor. The torque is constant, and therefore the traction force is also constant. The manufacturer always provides the highest constant traction force on the wheels resulting from the torque. When a critical speed is reached, the traction force decreases with increasing speed. Accordingly, the traction force is:

$$F_{tr,max} = \begin{cases} F_{tr,max}; & \forall 0 \leq v_{tr} \leq v_{cr} \\ F_{tr,max} = \frac{P_{tot}}{v_{tr}}; & \forall v_{cr} < v_{tr} \leq v_{max} \end{cases} \tag{5}$$

For acceleration, the train will use the maximum traction force; for cruising, the traction force will be equal to the total movement resistance forces; and for regenerative braking, it will use the maximum braking force (Figure 3).

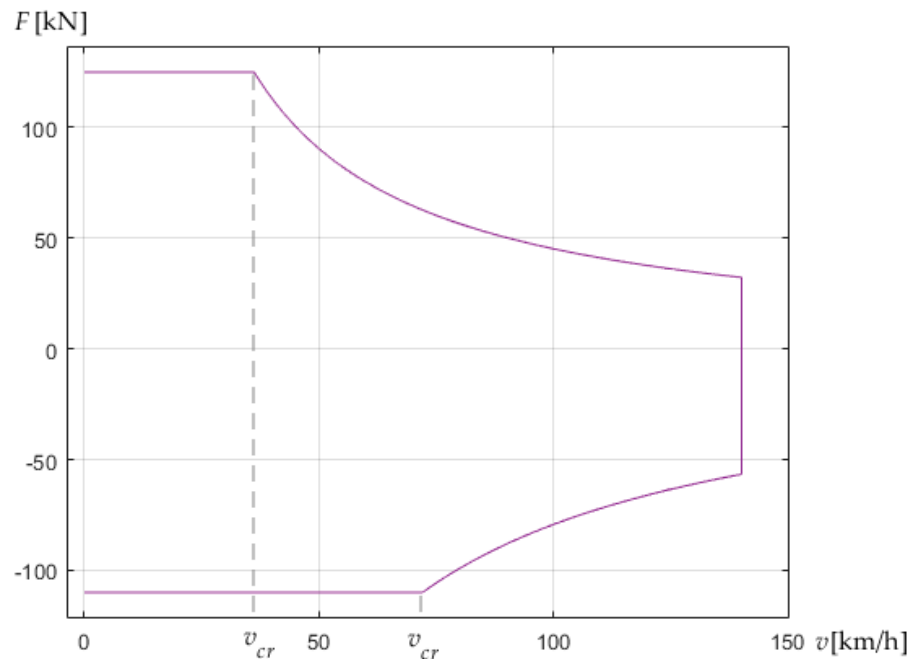


Figure 3. Traction properties of the train.

In Figure 4, the railway profile is depicted. The yellow line represents the gradient of the railway in ‰, the red line represents the speed limit, and the blue line represents train speed.

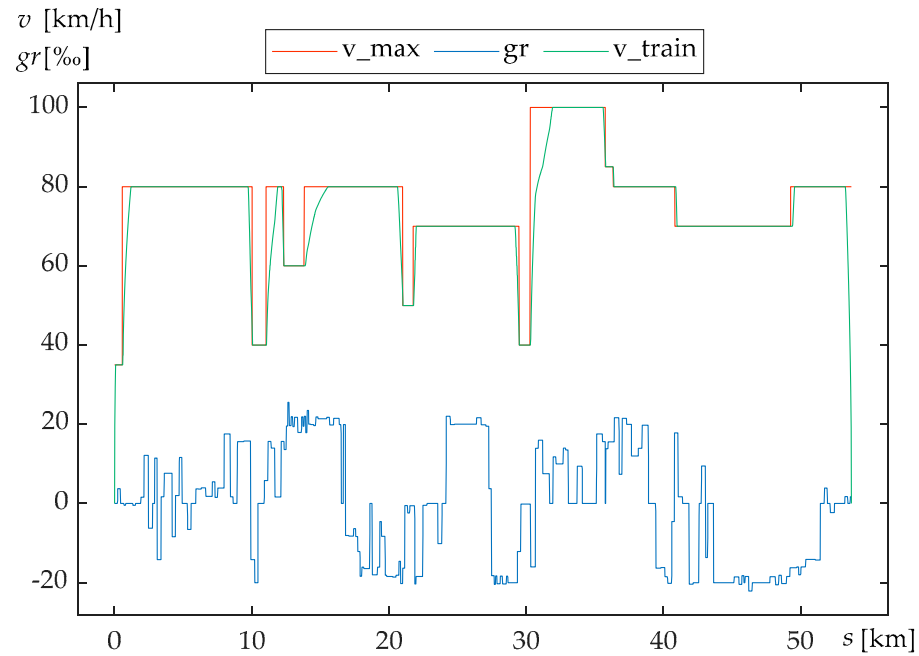


Figure 4. The railway profile.

In Figure 5, red line represents power demand, and green line represents resistance force of the railway.

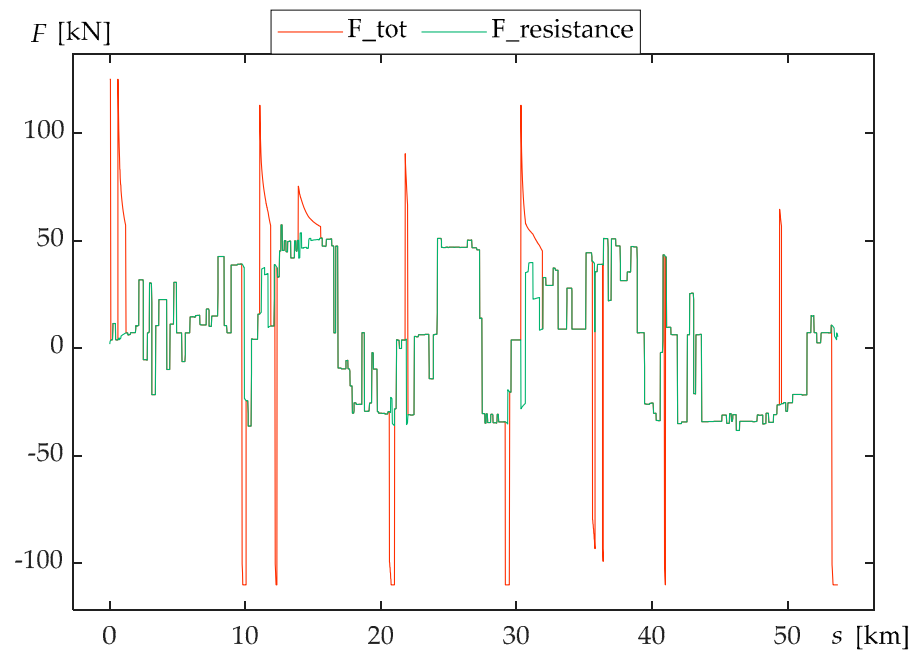


Figure 5. Demand force and the resistance force of the railway.

Based on the railway profile data depicted in Figure 5 and train parameters, resistance power and demand power were calculated. Figure 4 shows the calculated power distribution on the railway. Green line represents calculated resistance power, and red line represents the necessary traction power for the simulated train.

The railway is extremely hilly and full of radiuses, which thoroughly tests the endurance of all power sources and shows whether regenerative braking can store enough energy to make the system sustainable.

2.4. Fuel Cell

Fuel cells are devices that convert chemical energy into electrical energy. The fuel cell system contains a fuel supply system, an air supply system, a water management system, and a fuel cooling system. They include AFC (alkaline fuel cell), PEMFC (Polymer Electrolyte Membrane), DMFC (Direct Methanol), PAFC (Phosphoric Acid), MCFC (Molten Carbonate), and SOFC (Solid Oxide). Only PEMFC has zero harmful emissions of exhaust gases.

PEMFC operates at relatively low temperatures and has a high power density. It cannot change the output power very fast, so PEMFC has slow dynamics. This can be compensated by faster dynamics from storage devices. The voltage of one cell is about 1 V with a current density of 0.5 A/cm² to 1 A/cm². To obtain higher power, the cells are joined in stacks. The fuel is hydrogen, and pure oxygen or oxygen from the air can be used as an oxidant.

PEMFC can reach 1.3 kW/L power density, 0.6 kW/L system power density, and 0.6 kW/kg mass-specific power density. It operates at low temperatures and can be started and operated in sub-zero temperatures, although normal operating temperatures are 20–90 °C [21]. For the above reasons, PEMFC was chosen for this study, even though other cells exist.

The load power of the fuel cell stack is:

$$P_{fc} = U_{fc} \cdot I_{Load,fc} \tag{6}$$

$$P_{fc} = (E_{oc} - U_{act} - U_{ohm})I_{Load,fc} \tag{7}$$

where U_{fc} is the fuel cell stack voltage in V, $I_{Load,fc}$ is the fuel cell current load in A, E_{oc} is the open circuit voltage in V, U_{ohm} is the ohmic voltage drop in V, and U_{act} is the activation voltage drop in V [22].

2.5. Battery

Lithium iron phosphate (LiFePO₄) is the safest cathode material used for the high-power modules required in hybrid vehicles. The advantages of this type of battery are the theoretical specific capacity of 170 Ah/kg and greater thermal stability against the release of oxygen, which makes it safer and more tolerant under extreme operating conditions [23].

It can change the output power much faster than a fuel cell, so it can compensate for power in the fuel cell. In the nominal operating range of the battery, during discharge, the voltage changes slightly. When the rated capacity is discharged, the battery enters the operating range, where the battery voltage decreases rapidly.

The load power of the battery cell for discharging is:

$$P_b = U_b \cdot I_{Load,b} \tag{8}$$

$$P_b = (E_0 - K \frac{Q_b}{Q_b - I_{load,b} \cdot t} I_{load,b} \cdot t - K \frac{Q_b}{Q_b - I_{load,b} \cdot t} I_{load,b} - R_b \cdot I_{load,b} + A \cdot e^{(-B \cdot I_{load,b} \cdot t)}) I_{load,b} \tag{9}$$

where U_b is the battery cell voltage in V, E_0 is the constant voltage in V, K is the polarization constant or the polarization resistance in Ω , Q_b is the standard battery capacity in Ah, $I_{Load,b}$ is the battery current load in A, R_b is the battery internal resistance in Ω , A is the voltage drop during the exponential zone in V, and B is the exponential time inverse constant in Ah⁻¹.

The load power of battery for charging is:

$$P_b = (E_0 - K \frac{Q_b}{Q_b - I_{load,b} \cdot t} I_{load,b} \cdot t - K \frac{Q_b}{I_{load,b} \cdot t - 0.1Q_b} I_{load,b} - R_b \cdot I_{load,b} + A \cdot e^{(-B \cdot I_{load,b} \cdot t)}) I_{load,b} \tag{10}$$

State of charge is:

$$SOC_b = 1 - \frac{1}{Q_b} \int I_{Load,b} dt \tag{11}$$

2.6. Supercapacitor

Supercapacitor (EDCL, Electrochemical Double Layer Capacitors) is a device used for energy storage, and it has high energy and power densities, high efficiency (almost 95%), and long lifetime. The main property of supercapacitor is the possibility of rapid charging and discharging without loss of efficiency (>95%) during thousands of cycles [24].

Supercapacitors can be recharged in a very short time and have an excellent ability to change the output power very fast, faster than battery, and to operate with frequent peak power demands. All these reasons improve the efficiency of the vehicle and save energy, so they are suitable for installation. They especially show their excellent properties during regenerative braking.

The load power of the supercapacitor cell is:

$$P_{sc} = U_{sc} \cdot I_{Load,sc} \tag{12}$$

$$P_{sc} = (U_1 + R_1 \cdot I_{Load,sc}) \cdot I_{Load,sc} \tag{13}$$

$$P_{sc} = (\frac{-C_0 + \sqrt{C_0^2 + 2C_v \cdot Q_1}}{C_v} + R_1 \cdot I_{Load,sc}) \cdot I_{Load,sc} \tag{14}$$

where U_{sc} is the voltage of the supercapacitor cell in V, R_1 is the resistance of the supercapacitor's main cell in Ω , $I_{Load,sc}$ is the supercapacitor's load current in A, U_1 is the voltage of the supercapacitor's main cell in V, C_0 is the constant capacitance in F, C_v is the constant parameter in F/V, and Q_1 is the instantaneous charge in the supercapacitor's main cell in As.

State of charge is:

$$SOC_{sc} = 1 - \frac{1}{Q_{sc}} \int I_{Load,sc} dt \tag{15}$$

2.7. Method of Sequential Quadratic Programming

To solve the nonlinearity and non-convexity of the resulting optimal control problem, sequential quadratic programming is used [25]. SQP is used to optimally control the management of power sources with the aim of the lowest amount of fuel consumption.

The main objective function for minimization is:

$$\min f(x) = \int_{t_0}^{t_f} P_{tot}(v(t), s(t), u(t)) dt \tag{16}$$

where $v(t)$ is the speed of the train; $s(t)$ is the distance; and $u(t)$ is the set of all variables that affect driving, as shown by Equation (3).

To obtain the minimum fuel consumption, which is directly a function of energy, it is necessary to determine the discrete-time formulation of the problem. The problem of energy consumption is defined by hybridization ratios [26]. Minimization is achieved by composing a Quadratic Programming (QP) subproblem based on the quadratic approximation of the Lagrange function [27].

$$L(x, \lambda) = f(x) + \sum_{i=1}^m \lambda_i g_i(x) \tag{17}$$

where $f(x)$ is the main objective function, $g_i(x)$ are the inequality constraints, λ_i are Lagrange multipliers under the non-negativity constraint, and m is the total number of restrictions.

QP subproblem is given by

$$\begin{aligned} \min_{d \in \mathbb{R}^m} & \frac{1}{2}d^T H_k d + \nabla f(x_k)^T d \\ & \nabla g_i(x_k)^T d + g_i(x_k) = 0, \quad i = 1, \dots, m_e \\ & \nabla g_i(x_k)^T d + g_i(x_k) \leq 0, \quad i = m_e + 1, \dots, m \end{aligned} \tag{18}$$

where d is the number of iterations, H_k is the Hessian Matrix, and m_e is the equality constraints number. Updated, the Hessian Matrix is:

$$H_{k+1} = H_k + \frac{q_k q_k^T}{q_k^T s_k} - \frac{H_k s_k s_k^T H_k^T}{s_k^T H_k s_k} \tag{19}$$

where

$$\begin{aligned} s_{k+1} &= x_{k+1} - x_k \\ q_k &= (\nabla f(x_{k+1}) + \sum_{i=1}^m \lambda_i \nabla g_i(x_{k+1})) - (\nabla f(x_k) + \sum_{i=1}^m \lambda_i \nabla g_i(x_k)) \end{aligned} \tag{20}$$

Duration of the simulation in time, boundary conditions, and time-dependent constraints and control variables are:

$$g_i(x) = \begin{cases} I_{sc,\min} \leq I_{Load,sc} \leq I_{sc,\max} \\ I_{b,\min} \leq I_{Load,b} \leq I_{b,\max} \\ SOC_{sc,\min} \leq SOC_{sc} \leq SOC_{sc,\max} \\ SOC_{b,\min} \leq SOC_b \leq SOC_{b,\max} \\ hr_{sc,\min} \leq hr_{sc} \leq hr_{sc,\max} \\ hr_{b,\min} \leq hr_b \leq hr_{b,\max} \end{cases} \tag{21}$$

where $I_{Load,sc}$ is the discharge current of the supercapacitor, $I_{Load,b}$ is the discharge current of the battery, SOC_{sc} is the state of charge of the supercapacitor, SOC_b is the state of charge of the battery, hr_{sc} is the supercapacitor hybridization ratio, and hr_b is the battery hybridization ratio.

2.8. Model Parameters

In the simulation model, the PEMFC modules “Ballard” Fcvelocity-HD6, rechargeable LFP battery “Lithium Werks” 26650, and “Maxwell” supercapacitor BCAP3000 were used (Table 2). According to the proportion of hybridization, the power used to discharge the battery and the supercapacitor was determined. In the simulation model, it was set that the algorithm optimizes the discharge current and thus obtains the optimal hybridization ratio for both the battery and the supercapacitor. As a result, the optimal discharge current of both the battery and the supercapacitor was obtained. The load currents are:

$$I_{Load,sc} = \frac{hr_{sc} \cdot P_{tot}}{U_{sc} \cdot n_{par,sc} \cdot n_{ser,sc}} \tag{22}$$

$$I_{Load,b} = \frac{hr_b \cdot P_{tot}}{U_b \cdot n_{par,b} \cdot n_{ser,b}} \tag{23}$$

where $n_{par,sc}$ is the number of supercapacitor cells in parallel, $n_{ser,sc}$ is the number of supercapacitor cells in series, $n_{par,b}$ is the number of battery cells in parallel, $n_{ser,b}$ is the number of battery cells in series, and P_{tot} is demand power.

Table 2. Power sources properties.

Fuel Cell Stack			Battery Cell		
Rated power	P_{fc}	150 kW	Rated voltage	U_0	3.3 V
Idle power	$P_{fc,min}$	6 kW	Rated capacity	Q_0	2.56 Ah
Maximum load current	$I_{fc,max}$	320 A	Maximum charging current	$I_{ch,max}$	10 A
Mass	m_{fc}	404 kg	Maximum discharging current	$I_{dis,max}$	20 A
Average hydrogen consumption	m_{H2}	2.5 g/s	Mass	m_B	76 g
Supercapacitor Cell			Train		
Nominal capacitance	C_{sc}	3000 F	Tractive power	$P_{tr,max}$	1255 kW
Rated voltage	U_{sc}	2.7 V	Tractive force	$P_{tr,max}$	125 kN
Maximum discharging current	$I_{sc,max}$	160 A	Braking power	$P_{br,max}$	2200 kW
Mass	m_{sc}	506.7 g	Braking force	$P_{br,max}$	110 kN
			Mass	m_{tot}	191 t

The fuel cell stack load current is:

$$I_{Load,fc} = \frac{hr_{fc} \cdot P_{tot}}{U_{fc} \cdot n_{par,sc}} \tag{24}$$

where hr_{fc} is the fuel cell stack hybridization ratio, and $n_{par,fc}$ is the number of fuel cell stacks in parallel.

First, the optimization parameters with boundaries in the simulation and the objective function with the final desired value are selected (Figure 6).

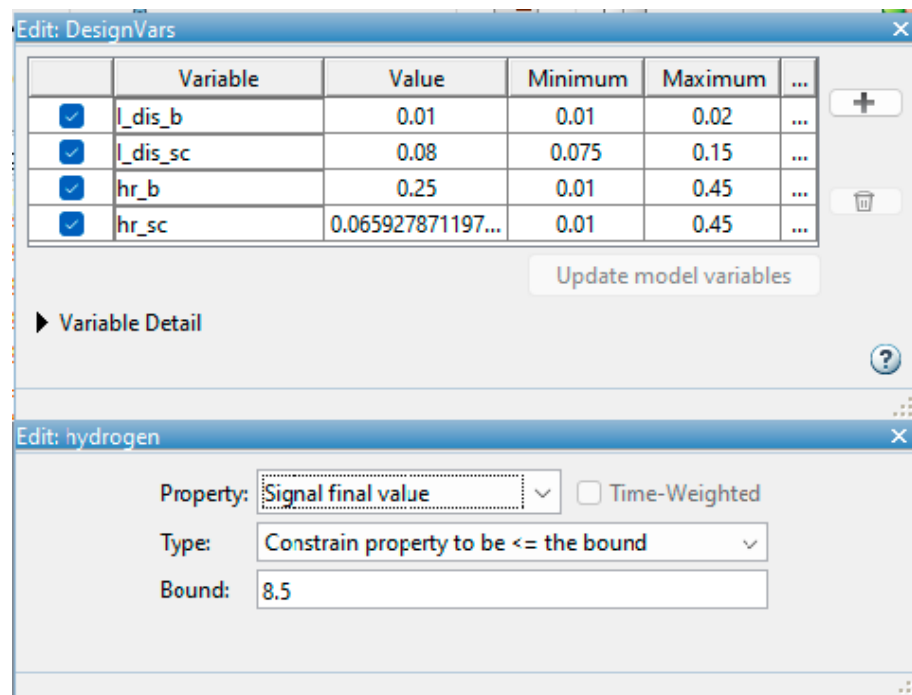


Figure 6. Setting of the main objective function, constraints, and boundaries (current in kA).

Boundaries for the hybridization ratio have been proven, and it has already been shown that with the ratio $hr_b/hr_{fc} = 0.33$, the vehicle can travel the most kilometers per kilogram of hydrogen. Since the supercapacitor also participates in traction, the upper boundary is 0.45 for both energy stores, as there is space for optimization. If the system does not converge, the values will expand [28].

Energy storages discharge current constraints are set according to the manufacturer’s datasheet.

3. Results and Discussion

In the simulation, randomly selected parameters were taken and then optimized. Simulation results are values for the battery hybridization ratio, supercapacitor hybridization ratio, battery discharge current, and supercapacitor discharge current. Optimal parameter values for the presented study were obtained through iteration (Table 3, Figure 7).

Table 3. Optimized parameters.

Parameter		Start	Optimized
Battery hybridization ratio	hr_b	0.25	0.39
Supercapacitor hybridization ratio	hr_{sc}	0.05	0.06592787
Battery discharge current	$I_{dis,b}$	0.01 kA	0.017 kA
Supercapacitor discharge current	$I_{dis,sc}$	0.090.08 kA	0.0801 kA

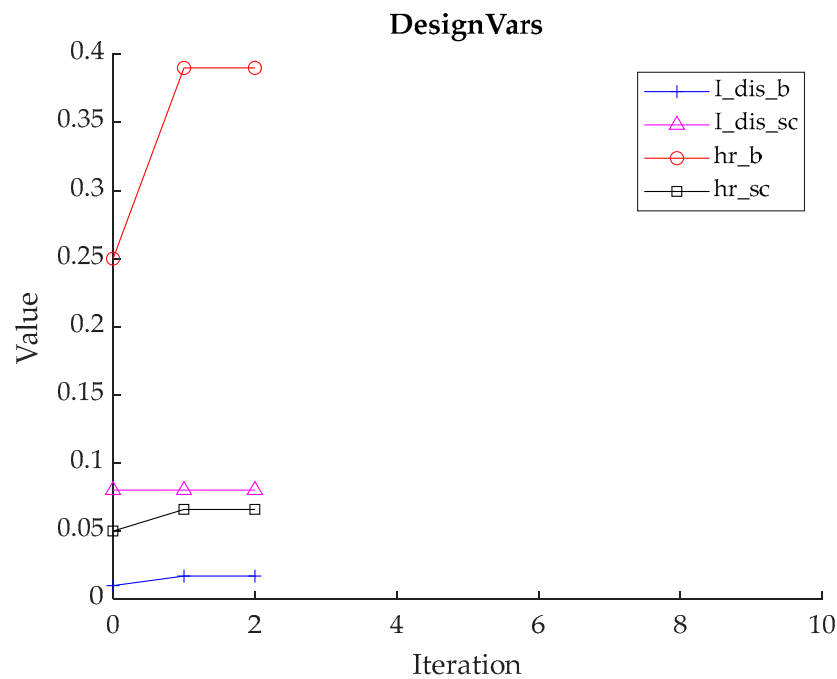


Figure 7. Iteration of parameters.

The optimal values were calculated through 2 iterations. Figure 7 depicts the iteration process.

With the optimal parameters for the proposed hybrid system, the consumption of hydrogen is 8 kg over a distance of 53.71 km, which the train travels in 2717 s. During acceleration or when driving uphill, energy management uses the power of the fuel cell, the battery, and the supercapacitor together. When cruising, the supercapacitor is first completely discharged, and then the battery is used. In order not to discharge both the battery and the supercapacitor at the same time, energy management determines the optimal hybridization ratio. Likewise, if only the supercapacitor is pulling the train, the

fuel cell charges the battery. The hybridization ratio of the fuel cell is obtained by $hr_{fc} = 1 - hr_b - hr_{sc}$, which determines the power of the fuel cell and can be said to be optimal.

All that data can be graphically shown with the presented simulation model. Figure 8 shows the difference in hydrogen consumption for randomly selected and optimized parameters of the propulsion system. The optimized solution yields a decrease in fuel consumption of 14.7%. That is a saving of 1.373 kg of hydrogen compared to the initial solution.

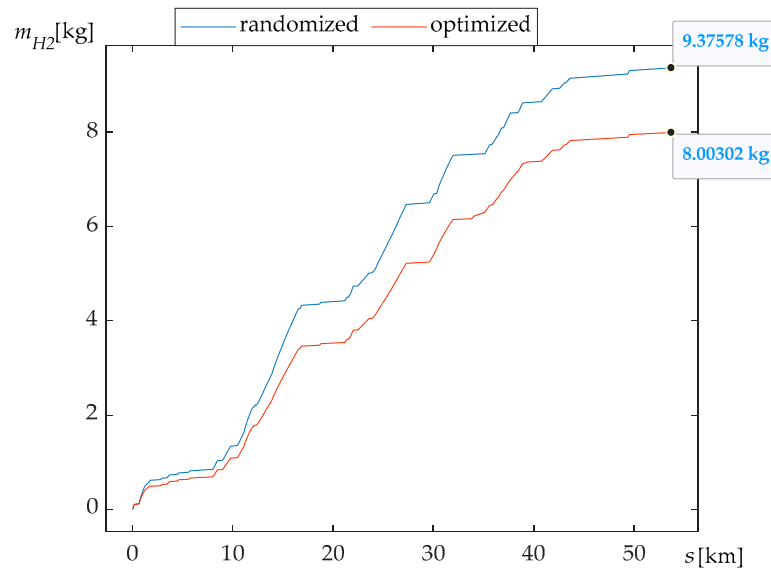


Figure 8. Consumption of the hydrogen (red is optimized, blue is randomized).

Since hydrogen consumption is a consequence of energy consumption, the consumed energy for the optimized solution is 216.99 kWh (Figure 9). Compared to the initial solution of 283.15 kWh, the optimized system results in a decrease in energy consumption of 23.37%. Due to the optimal selection of parameters and energy management that uses power sources according to given conditions, savings are possible. The profile of the railway with pronounced uphill and downhill enables regenerative braking, which is optimally used to discharge and charge the energy storage and thus save energy (Figure 10).

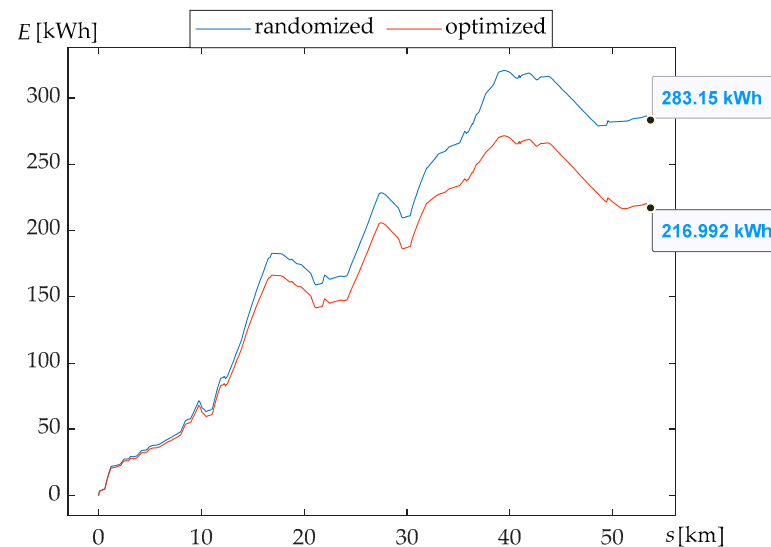


Figure 9. Demand of the energy (red is optimized, blue is randomized).

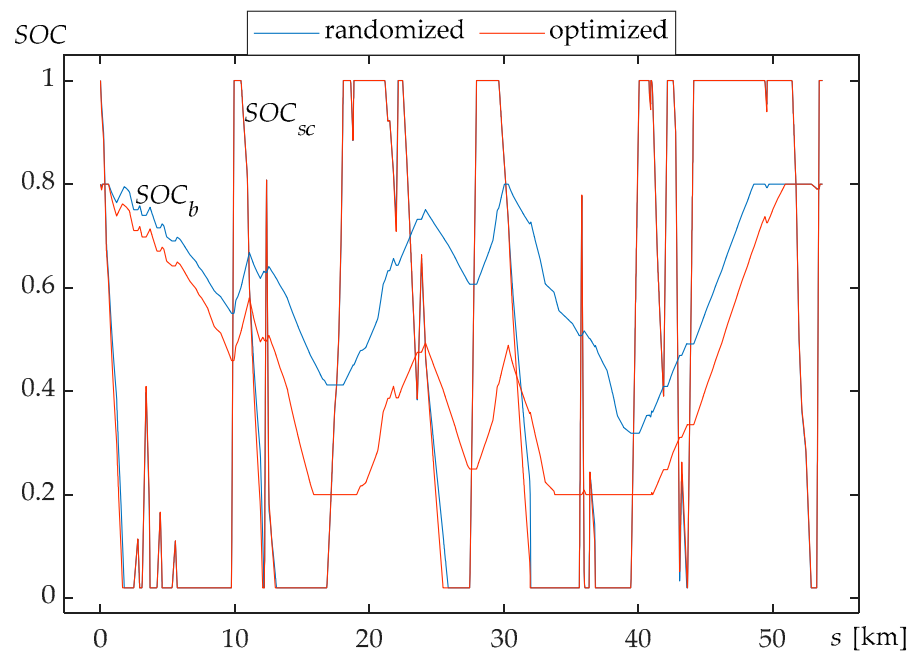


Figure 10. SOC of the battery and the supercapacitor (red is optimized, blue is randomized).

Due to the different losses in the devices, according to the hybridization ratios, the total power of all power sources will not always be the same. Consequently, with the optimal hybridization ratio, a lower required total power to propel the train was achieved. By comparing the required train power on the modeled railway for the initial and optimized drive system, this was revealed during acceleration and regenerative braking (Figure 11).

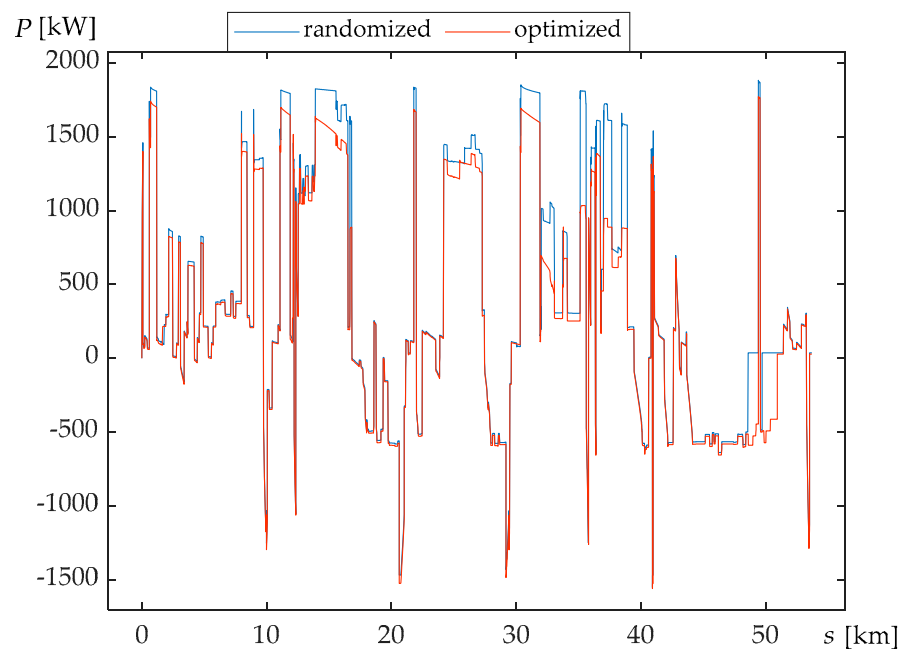


Figure 11. Demand for power (red is optimized, blue is randomized).

According to all losses, the highest power of all power sources is 1772 kW. According to the optimal hybridization ratio, the fuel cell consumes 964 kW. This power requires 7 stacks of fuel cells, which have a total mass of 2828 kg. The fuel cell with 7 stacks has 1050 kW, which means that the rest of the optimal value is used to propel auxiliary devices.

Since the hybridization ratio and discharge current of the battery package are found through optimization, the battery package has a power of 691 kW. The operating voltage of each power source is 800 V, so 243 cells will be connected in series in the battery package. According to the discharge current in the battery package, 52 cells will be connected in parallel. The mass is 960 kg.

The same types of parameters affect the supercapacitor. According to the operating voltage, 296 cells are connected in series in a supercapacitor package. By optimizing the hybridization ratio and the discharge current, the supercapacitor package has a power of 117 kW, and 2 cells are connected in parallel. According to this connection, the mass is 302 kg.

4. Conclusions

This paper presents the development of a hybrid power train system with fuel cells and presents the parameters of each component. A new energy management strategy based on railway loads and the state of charge of the energy storage is proposed. Then, the system was optimized using the SQP method, and the hydrogen consumption was calculated. By optimizing using Matlab/Simulink, it was shown that the mass of the train and the consumption of hydrogen could be reduced.

Because the railway is sharp and demanding, the energy management had to be different than what is usually set. Big uphill transits consume a lot of energy, but traveling downhill can be used for energy regeneration, which is why supercapacitor charging is used when traveling downhill, while the battery is charged via the fuel cell only when the supercapacitor conducts the traction itself. Nevertheless, the simulation showed that the train could overcome such a railway and, at the same time, find the lowest hydrogen consumption with optimal hybridization parameters and discharge currents. The result is a 14.7% decrease in hydrogen fuel consumption and 23.37% less energy consumed.

The current fuel cell systems do not leave much space for optimization. Only by optimally choosing the hybridization ratios of the battery and the supercapacitor can the power of the fuel cell be said to be optimal. The batteries and supercapacitors are delivered in smaller cells, and they give the possibility of optimization.

On the existing train prototype, the total mass of 3 diesel engines and 3 alternators is around 7300 kg. By optimizing the hybrid train with fuel cells, the mass of the power sources (including converters and inverter) was obtained at less than 4091 kg, which indicates that a fuel cell hybrid train is favorable for mass reduction. Therefore, it can be argued that a fuel cell hybrid train can have the same acceleration as a diesel train, which is important in passenger traffic.

The presented simulation model could be a useful tool in the conceptual development phase of future hybrid train propulsion systems and train modifications and shorten the development time of future environmentally friendly railway systems.

Author Contributions: Conceptualization, M.M.; methodology, R.T.; software, M.M.; validation, M.S., M.L. and R.T.; formal analysis, R.T.; investigation, M.M.; writing—original draft preparation, M.M.; writing—review and editing, M.S. and R.T.; visualization, M.L.; All authors have read and agreed to the published version of the manuscript.

Funding: This research received no external funding.

Institutional Review Board Statement: Not applicable.

Informed Consent Statement: Not applicable.

Data Availability Statement: Battery: <https://lithiumwerks.com/> (accessed on 1 February 2023). Supercapacitor: <https://maxwell.com/products/ultracapacitors/> (accessed on 1 February 2023). Fuel cell: <https://www.ballard.com/> (accessed on 1 February 2023).

Conflicts of Interest: The authors declare no conflict of interest.

References

1. Cui, Z.; Chen, J.; Li, C.; Yin, Y.; Hao, M. The Calculation and Analysis of Carbon Emission in Traction Power Supply System of High-Speed Rail. *Tech. Gaz.* **2023**, *30*, 226–234.
2. Shang, W.; Yu, S.; Zhang, G.; Li, Q.; Chen, W. Fuel cell hybrid locomotive system based on equivalent consumption minimization strategy. In Proceedings of the Chinese Automation Con-Gress (CAC), Jinan, China, 20–22 October 2017. [CrossRef]
3. Abdelrahman, A.; Attia, Y.; Woronowicz, K.; Youssef, M. Hybrid Fuel Cell/Battery Rail Car: A Feasibility Study. *IEEE Trans. Transp. Electrification* **2016**, *2*, 493–503. [CrossRef]
4. International Union of Railways. *UIC Code 624-Exhaust Emission Tests for Diesel Traction Engines*; International Union of Railways: Paris, France, 2017; ISBN 978-2-7461-2575-9.
5. Sumpavakup, C.; Kulworawanichpong, T. Multi-Train Movement Simulation Using MATLAB Object-Oriented Programming. *Appl. Mech. Mater.* **2015**, *763*, 153–158. [CrossRef]
6. Sarma, U.; Ganguly, S. Modelling and cost-benefit analysis of PEM fuel-cell-battery hybrid energy system for locomotive application. In Proceedings of the Technologies for Smart-City Energy Security and Power (ICSESP), Bhubaneswar, India, 28–30 March 2018.
7. Saw, L.; Somasundaram, K.; Ye, Y.; Tay, A. Electro-thermal analysis of Lithium Iron Phosphate battery for electric vehicles. *J. Power Sources* **2014**, *249*, 231–238. [CrossRef]
8. Tsukahara, K.; Kondo, K. A study on methods to design and select energy storage devices for Fuel Cell hybrid powered railway vehicles. In Proceedings of the 39th Annual Conference of the IEEE Industrial Electronics Society, Vienna, Austria, 10–13 November 2013.
9. Guo, L.; Yedavalli, K.; Zinger, D. Design and modeling of power system for a fuel cell hybrid switcher locomotive. *Energy Convers. Manag.* **2011**, *52*, 1406–1413. [CrossRef]
10. Malvezzi, M.; Pugi, L.; Conti, R.; Toni, P.; Tesi, S.; Meli, E.; Rindi, A. A Tool for Prediction and Optimization of Railway Traction Systems with Respect to an Expected Mission Profile. *Chem. Eng. Trans.* **2013**, *33*, 7.
11. Angalaeswari, S.; Jamuna, K. Optimal Energy Management Using Sequential Quadratic Programming Algorithm for Stand Alone PV System. *Int. J. Appl. Eng. Res.* **2017**, *12*, 12250–12255.
12. Liu, X.; Xun, J.; Ning, B.; Liu, T.; Xiao, X. Moving Horizon Optimization of Train Speed Profile Based on Sequential Quadratic Programming. In Proceedings of the International Conference on Intelligent Rail Transportation (ICIRT), Singapore, 12–14 December 2018.
13. Khalik, Z.; Padilla, G.; Romijn, T.; Donkers, M. Vehicle Energy Management with Ecodriving: A Sequential Quadratic Programming Approach with Dual Decomposition. In Proceedings of the Annual American Control Conference (ACC), Milwaukee, WI, USA, 27–29 June 2018.
14. Ning, Q.; Xuan, D.; Nan, Y.; Kim, Y. Modeling and Simulation for Fuel Cell-Battery Hybrid Electric Vehicle. In Proceedings of the International Conference on Computer Modeling and Simulation, Washington, DC, USA, 20–22 February 2009.
15. Barbir, F. *PEM Fuel Cells: Theory and Practice*; Elsevier Inc.: Waltham, MA, USA, 2013.
16. *Croatian Railways-Infrastructure, Izveštje o Mreži*; Croatian Railways-Infrastructure: Zagreb, Croatia, 2022.
17. Furuta, R.; Kawasaki, J.; Kondo, K. Hybrid Traction Technologies with Energy Storage Devices for Nonelectrified Railway Lines. *IEEE Trans. Electr. Electron. Eng.* **2010**, *5*, 291–297. [CrossRef]
18. Sehrili, E.; Cetinceviz, Y. Comparison of Average Current Controlled PFC SEPIC and CUK Converter Feeding Current Controlled SRM. *Tech. Gaz.* **2020**, *29*, 1789–1795. [CrossRef]
19. Lai, C.-M. Development of a Novel Bidirectional DC/DC Converter Topology with High Voltage Conversion Ratio for Electric Vehicles and DC-Microgrids. *Energies* **2016**, *9*, 410. [CrossRef]
20. Serdar, J. *Lokomotive-Opci Dio*; Sveucilisna Naklada Liber: Zagreb, Croatia, 1977.
21. Mench, M. *Fuel Cell Engines*; John Wiley & Sons, Inc.: Hoboken, NY, USA, 2008.
22. Hong, Z.; Han, Y.; Li, Q.; Chen, W. Design of Energy Management System for Fuel Cell/Supercapacitor Hybrid Locomotive. In Proceedings of the IEEE Vehicle Power and Propulsion Conference (VPPC), Hangzhou, China, 17–20 October 2016. [CrossRef]
23. Beninati, S.; Damen, L.; Mastragostino, M. Fast sol-gel synthesis of LiFePO₄/C for high power lithium-ion batteries for hybrid electric vehicle application. *J. Power Sources* **2009**, *194*, 1094–1098. [CrossRef]
24. Tashima, D.; Samantara, A. *Supercapacitors for the Next Generation*; IntechOpen: London, UK, 2022.
25. Kyoungcheol, O.; Jeongmin, K.; Dongho, K.; Donghoon, C.; Hyunsoo, K. Optimal power distribution control for parallel hybrid electric vehicles. In Proceedings of the IEEE International Conference on Vehicular Electronics and Safety, Xi'an, China, 14–16 October 2005.
26. Ghandriz, T.; Jacobson, B.; Murgovski, N.; Nilsson, P.; Laine, L. Real-Time Predictive Energy Management of Hybrid Electric Heavy Vehicles by Sequential Programming. *IEEE Trans. Veh. Technol.* **2021**, *70*, 4113–4128. [CrossRef]

27. Shivappriya, S.N.; Karthikeyan, S.; Prabu, S.; Pérez de Prado, R.; Parameshachari, B.D. A Modified ABC-SQP-Based Combined Approach for the Optimization of a Parallel Hybrid Electric Vehicle. *Energies* **2020**, *13*, 4529. [[CrossRef](#)]
28. Jeong, K.; Oh, B. Fuel economy and life-cycle cost analysis of a fuel cell hybrid vehicle. *J. Power Sources* **2022**, *105*, 58–65. [[CrossRef](#)]

Disclaimer/Publisher's Note: The statements, opinions and data contained in all publications are solely those of the individual author(s) and contributor(s) and not of MDPI and/or the editor(s). MDPI and/or the editor(s) disclaim responsibility for any injury to people or property resulting from any ideas, methods, instructions or products referred to in the content.